MOLECULAR AND CELLULAR BIOLOGY, Jan. 2009, p. 31–42 Vol. 29, No. 1
0270-7306/09/$08.00+0 doi:10.1128/MCB.00776-08

Studies of the 5′ Exonuclease and Endonuclease Activities of CPSF-73 in Histone Pre-mRNA Processing▽†

Xiao-cui Yang, Kelly D. Sullivan, William F. Marzluff, and Zbigniew Dominski*

Department of Biochemistry and Biophysics and Program in Molecular Biology and Biotechnology, University of North Carolina at Chapel Hill, Chapel Hill, North Carolina 27599

Received 14 May 2008/Returned for modification 9 July 2008/Accepted 15 October 2008

Processing of histone pre-mRNA requires a single 3′ endonucleolytic cleavage guided by the U7 snRNP that binds downstream of the cleavage site. Following cleavage, the downstream cleavage product (DCP) is rapidly degraded in vitro by a nuclease that also depends on the U7 snRNP. Our previous studies demonstrated that the endonucleolytic cleavage is catalyzed by the cleavage/polyadenylation factor CPSF-73. Here, by using RNA substrates with different nucleotide modifications, we characterize the activity that degrades the DCP. We show that the degradation is blocked by a 2′-*O*-methyl nucleotide and occurs in the 5′-to-3′ direction. The U7-dependent 5′ exonuclease activity is processive and continues degrading the DCP substrate even after complete removal of the U7-binding site. Thus, U7 snRNP is required only to initiate the degradation. UV cross-linking studies demonstrate that the DCP and its 5′-truncated version specifically interact with CPSF-73, strongly suggesting that in vitro, the same protein is responsible for the endonucleolytic cleavage of histone pre-mRNA and the subsequent degradation of the DCP. By using various RNA substrates, we define important space requirements upstream and downstream of the cleavage site that dictate whether CPSF-73 functions as an endonuclease or a 5′ exonuclease. RNA interference experiments with HeLa cells indicate that degradation of the DCP does not depend on the Xrn2 5′ exonuclease, suggesting that CPSF-73 degrades the DCP both in vitro and in vivo.

3′-end processing is an essential step in converting eukaryotic mRNA precursors (pre-mRNAs) to mature mRNAs. Metazoan pre-mRNAs are processed at the 3′ end by two distinct mechanisms (40). The vast majority of mRNA precursors are processed by cleavage coupled to polyadenylation. This mechanism depends on the presence of two sequence elements in the precursor: a highly conserved polyadenylation signal (AAUAAA) and a less conserved, G/U-rich downstream element (6). Cleavage occurs between the two sequence elements, usually about 20 nucleotides 3′ to the AAUAAA signal. The upstream cleavage product is subsequently polyadenylated. Cleavage/polyadenylation is executed by a large complex composed of at least 12 proteins. The AAUAAA signal interacts with a 5-subunit cleavage/polyadenylation specificity factor (CPSF) (17), whereas the G/U-rich downstream element interacts with a 3-subunit cleavage stimulation factor (CstF) (6). Among other proteins, the cleavage/polyadenylation machinery also includes poly(A) polymerase, which catalyzes the addition of the poly(A) tail (6), and symplekin, which plays a yet-uncharacterized role in 3′-end processing (36). Increasing numbers of both genetic and biochemical studies indicate that endonucleolytic cleavage that proceeds polyadenylation is carried out by CPSF-73, the 73-kDa subunit of CPSF (23, 30). CPSF-73 is a member of the metallo-β-lactamase family of mostly hydrolytic enzymes that utilize zinc ions during catalysis (1, 4). A small group of the metallo-β-lactamase proteins function in metabolism of DNA and RNA substrates as endonucleases and/or 5′-to-3′ exonucleases (4, 9, 24).

A distinct 3′-end processing mechanism operates on metazoan replication-dependent histone pre-mRNAs (10). These transcripts are cleaved between a highly conserved stem-loop structure and a purine-rich histone downstream element (HDE) directly producing the mature histone mRNAs that end with the stem-loop followed by a 5-nucleotide single-stranded tail. 3′-end processing of histone pre-mRNAs critically depends on the HDE, which interacts with U7 snRNP. The interaction is mediated by formation of a double-stranded RNA between the HDE and the 5′ end of U7 snRNA, an approximately 60-nucleotide component of the U7 snRNP. The U7 snRNP contains an unusual Sm complex, in which the Sm proteins D1 and D2 are replaced by two related proteins: Lsm10 and Lsm11 (27, 28). The stem-loop structure forms a tight complex with the stem-loop binding protein. The stem-loop binding protein also binds a 100-kDa zinc finger protein (ZFP100), which in turn interacts with Lsm11. This bridging interaction is believed to stabilize U7 snRNP on the HDE (10). In common with cleavage/polyadenylation, 3′-end processing of histone pre-mRNAs also involves symplekin, although its role remains to be elucidated (19).

UV cross-linking studies demonstrated that the cleavage site in histone pre-mRNAs interacts in a U7-dependent manner with CPSF-73, thus strongly suggesting that the same endonuclease functions in generation of both polyadenylated and nonadenylated (histone) mRNAs (11). Following the in vitro cleavage reaction, the downstream product containing the HDE is rapidly degraded to mononucleotides by a nuclease that also depends on the U7 snRNA, giving rise to mononucle-

* Corresponding author. Mailing address: Program in Molecular Biology and Biotechnology, CB #3280, University of North Carolina, Chapel Hill, NC 27599. Phone: (919) 843-0307. Fax: (919) 962-1274. E-mail: dominski@med.unc.edu.

† Supplemental material for this article may be found at http://mcb.asm.org/.

▽ Published ahead of print on 27 October 2008.

otides (11). Our preliminary data suggested that also this reaction is catalyzed by CPSF-73 (11).

In this study, we show that degradation of the downstream cleavage product (DCP) is a result of a processive 5′-to-3′ exonuclease activity and further support the involvement of CPSF-73. We also show that the position of the HDE relative to the 5′ end of the transcript determines whether cleavage is endonucleolytic or exonucleolytic and provide in vivo data suggesting that degradation of the DCP formed after 3′-end processing of histone pre-mRNA does not require Xrn2.

MATERIALS AND METHODS

Preparation and labeling of RNA substrates. Most RNAs were synthesized in Dharmacon (Lafayette, CO) and, depending on the quality of synthesis, were used either directly or gel purified to isolate the full-length product. RNA substrates containing a single internal label were constructed by ligating two RNA fragments by using DNA ligase and a bridging oligonucleotide, essentially as described previously (25). Prior to ligation, the downstream fragment was labeled at the 5′ end with ^{32}P by using T4 polynucleotide kinase, as described previously (11). All RNA substrates were named based on the number of nucleotides present in front of the DCP, for example, DCP, DCP+5, or DCP−2. The names of the substrates containing a single internal label additionally reflected the position of a modified nucleotide relative to the DCP sequence: 2′-*O*-methyl (m), deoxy (d), or phosphorothioate (s). The DCP+10 and DCP+15 substrates were constructed by ligating the 5′ end of the DCP−9/s substrate to 19- and 24-nucleotide RNA fragments, respectively. The ligation products were gel purified, quantified, and labeled at the 5′ end with ^{32}P by using T4 polynucleotide kinase. The internally labeled 86-nucleotide H2a pre-mRNA containing the stem-loop structure and the HDE was synthesized by T7 transcription in the presence of [α-^{32}P]UTP, as described previously (13).

Preparation of nuclear extracts and RNA processing and degradation. Nuclear extracts were prepared from mouse myeloma cells, as described previously (13). Unless otherwise indicated, all processing and degradation reactions were carried out for 90 min in the presence of 20 mM EDTA, as described previously (13). The efficiency of degradation was calculated by comparing the amount of the released radioactive mononucleotide to the amount of the input substrate used in the reaction. The U7 dependence of processing and degradation reactions was determined by using 100 ng of an anti-M oligonucleotide that is complementary to the first 17 nucleotides of the mammalian U7 snRNA (11). A 2′-*O*-methyl anti-D oligonucleotide directed to the first 19 nucleotides of the *Drosophila* U7 snRNA was used at the same concentration as a negative control (11). In some reactions, the U7 dependence was also confirmed by using 500 ng (a 1,000-fold excess relative to the labeled substrate) of an RNA containing the wild-type sequence of the HDE (wtHDE RNA). A corresponding RNA containing a 4-nucleotide mutation replacing the AAGA sequence with UUCU within the HDE (mutHDE) was used at the same concentration as a negative control. Processing and degradation reactions were inhibited by NP-40 at a final concentration of 0.05%.

Analysis of processing products. After 90 min of incubation, processing reaction mixtures were treated for 1 h with proteinase K at 0.5 μg/μl, diluted 5× with a 7 M urea dye, and analyzed in low-resolution 8% polyacrylamide-7 M urea gels to asses the reaction efficiency. The same samples were additionally analyzed in high-resolution gels allowing separation of fragments that differ by 1 nucleotide. Mononucleotides containing a phosphate at the 5′ end were identified by electrophoresis in 12% gels based on comigration with mononucleotides generated by S1 nuclease, which leaves a 5′ phosphate, or products of KOH hydrolysis, which migrate 0.5 nucleotides faster due to the presence of an additional phosphate at the 3′ end. The lengths of larger products were determined with high-resolution 8% gels by comparison with appropriate size markers containing the same sequence (5′-labeled RNAs used for ligation) or with products of partial KOH hydrolysis. In other cases, the lengths of final processing products were determined by comparison with the lengths of processing intermediates generated due to random stalling of the U7-dependent exonuclease at each nucleotide.

UV cross-linking and immunoprecipitation. UV cross-linking experiments were carried out as previously described (11). Processing reaction mixtures were prepared in a final volume of 20 μl (equivalent to two regular reaction mixtures) and additionally contained 10 μg of *Saccharomyces cerevisiae* tRNA (Invitrogen) to reduce the amount of nonspecifically cross-linked proteins. Each processing reaction mixture was incubated for 10 min at 32°C to initiate the degradation process, and a 15-μl aliquot was exposed at room temperature to 1 J of UV while the remaining portion of the reaction mixture was incubated for additional 80 min to asses the extent of degradation. Following UV irradiation, reaction samples were treated for 5 h with RNase A and proteins resolved by electrophoresis in a sodium dodecyl sulfate (SDS)-polyacrylamide gel. Immunoprecipitation with anti-CPSF-73 (a gift from D. Bentley) was carried out under denaturing conditions, as described previously (11).

RNAi. RNA interference (RNAi) was performed using a two-hit method. Briefly, 7×10^6 HeLa cells were plated into 24-well plates and transfected with 3 μl of 20 μM stock small interfering RNAs (siRNAs) (Xrn2-1, Xrn2-2, or a combination of both) 24 h later. A day after the first siRNA treatment, cells were split 1:3 into six-well plates and after another 24 h were retransfected with 4 μl of siRNA. Seventy-two hours after the second transfection, samples were collected by addition of either Trizol (Invitrogen) or NP-40 lysis buffer directly to the wells. The siRNA target sequences in the human Xrn2 mRNA were GGG AAGAAAUAUUGGCAA (Xrn2-1) and AAGAGUACAGAUGAUCAUG (Xrn2-2).

Quantitative reverse transcription-PCR (qRT-PCR). Total cell RNA (2.5 μg) was treated with DNase (Promega), and reverse transcription reactions were performed with Moloney murine leukemia virus-reverse transcriptase (Invitrogen) using random hexamers to prime the cDNA. cDNA from the reaction was added directly to quantitative PCR reaction mixtures containing 2× Sybr green PCR master mix (Applied Biosystems) and oligonucleotide primers. PCR was performed using a 7900HT PCR system (Applied Biosystems), and data were analyzed using SDS 3.2 software (Applied Biosystems). Relative stability values were calculated using $\Delta\Delta C_T$ values generated using the equation $(C_T\text{siRNA}_{\text{Downstream}} - C_T\text{siRNA}_{3'\text{End}}) - (C_T\text{Control}_{\text{Downstream}} - C_T\text{Control}_{3'\text{End}})$, where $C_T\text{siRNA}_{\text{Downstream}}$ and $C_T\text{siRNA}_{3'\text{End}}$ represent threshold cycle (C_T) values for a given siRNA-treated sample amplified with the indicated primer set and $C_T\text{Control}_{\text{Downstream}}$ and $C_T\text{Control}_{3'\text{End}}$ represent C_T values for control-treated samples amplified using the same indicated primer set. The oligonucleotide primers used were as follows: Hist2H2AA 3′ End F (GGAGCAGTACGGCCTGGAT), Hist2H2AA 3′ End R (CGACG AGGAACTGAACAAGCT), Hist2H2AA #1 Downstream F (GGGACCCA CTCATCGAAGAG), Hist2H2AA #1 Downstream R (CGCGCCGTCTTC CATCT), Hist2H2AA #2 Downstream F (CCAGGGCGCTTTGGAAA), Hist2H2AA #2 Downstream R (GAGCTGGGTCTTGGCTTCAC), GAPDH 3′ End F (CCGCACCTTGTCATGTACCA), GAPDH 3′ End R (CCCTAGAATAAGACAGGACAAGTAACTG), GAPDH Downstream F (TCGCTCCAGTCCTAGGCTATCT), and GAPDH Downstream R (GGCT GCCCACAGAATAGCTT).

RESULTS

U7-dependent degradation of the DCP+1 substrate containing a site-specific radioactive phosphate. To study 3′-end processing of histone pre-mRNAs in vitro, we use an 86-nucleotide derivative of the mouse H2a-614 pre-mRNA that contains all necessary processing elements, including the stem-loop and the HDE (Fig. 1A). The H2a substrate labeled by random incorporation with [^{32}P]UTP is processed in a mouse nuclear extract to an upstream cleavage product containing the stem-loop and to 5′ monophosphate nucleosides that result from the degradation of the DCP (Fig. 1B, lane 2) (11). 3′-end processing of histone pre-mRNAs proceeds in the presence of 20 mM EDTA, which inhibits virtually all nonspecific nucleases present in the mouse nuclear extract. Blocking the 5′ end of the U7 snRNA by a complementary 2′-*O*-methyl oligonucleotide (anti-M) at 10 ng/μl prevents binding of the U7 snRNP to the RNA substrate and abolishes processing (Fig. 1B, lane 3). A 2′-*O*-methyl oligonucleotide with an unrelated sequence targeted to the 5′ end of the *Drosophila* U7 snRNA (anti-D), routinely used at the same concentration to measure the extent of nonspecific effects, does not affect processing (not shown). A synthetic RNA substrate with a sequence corresponding to the DCP or extended at the 5′ end by 1 or more nucleotides is also degraded in a U7-dependent manner in nuclear extracts from

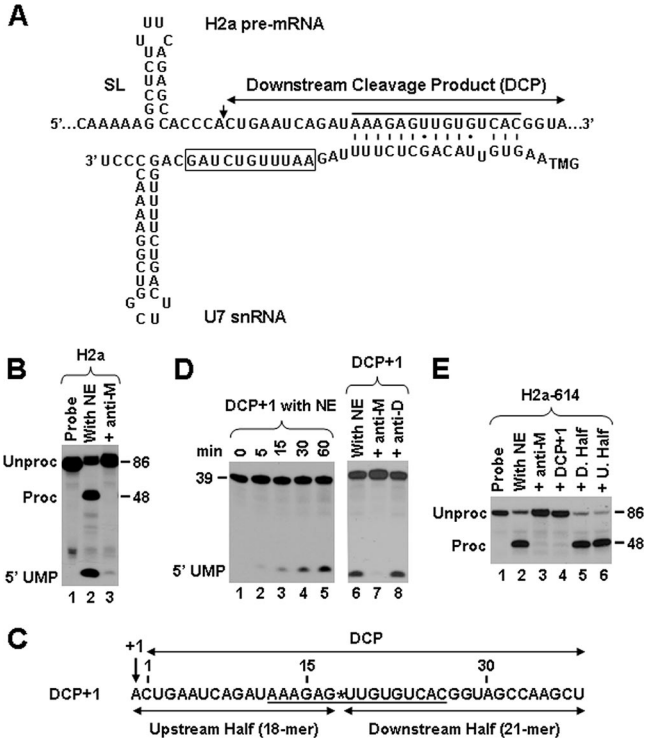

FIG. 1. U7-dependent degradation of the DCP generated during 3′-end processing of histone pre-mRNAs. (A) Fragment of the 86-nucleotide mouse histone H2a pre-mRNA substrate encompassing processing elements (top sequence) and the base pair interaction between the HDE (indicated with a thick line) and the U7 snRNA (bottom sequence). The cleavage site and the DCP are indicated with an arrowhead and a double-arrowed line, respectively. The Sm site in the U7 snRNA is indicated with a box. (B) In vitro processing of the internally labeled 86-nucleotide H2a substrate in a mouse nuclear extract (NE) under control conditions (lane 2) or in the presence of an oligonucleotide blocking the U7 snRNA (anti-M; lane 3). Lane 1 contains the unprocessed input pre-mRNA (Unproc). The 48-nucleotide processing product (Proc) results from cleavage of the input after the fifth nucleotide 3′ of the stem-loop. (C) The sequence of the DCP+1 RNA containing a single radioactive phosphate between nucleotides 17 and 18 of the DCP sequence (see Materials and Methods for the terminology used to designate RNA substrates). The DCP+1 RNA was constructed by ligating the upstream and the downstream halves, with the downstream half containing the radioactive phosphate at the 5′ end (indicated with an asterisk). The HDE interacting with the U7 snRNA is underlined. (D) Sixty-minute time course of the U7-dependent degradation of the DCP+1 RNA in a mouse nuclear extract (lanes 1 to 5) and the effect of an oligonucleotide blocking either the mouse U7 snRNA (anti-M; lane 7) or *Drosophila* U7 snRNA, used as a nonspecific control (anti-D; lane 8). (E) In vitro processing of the 5′-labeled H2a-614 pre-mRNA either under control conditions (lane 2) or in the presence of a 1,000-fold molar excess of RNA competitors containing either complete (lane 4) or partial (lanes 5 and 6) HDE. The processing shown in lane 3 was carried out in the presence of the anti-M oligonucleotide.

mammalian (11, 38) and *Drosophila* (12) cells. Thus, the degradation of the DCP can be uncoupled from the endonucleolytic cleavage of histone pre-mRNA.

In our previous studies, we used a DCP+1 RNA labeled at the 5′ end with a radioactive phosphate (11). The U7-dependent degradation of this substrate was monitored by the accumulation of ^{32}P-labeled mononucleotides. Since substrates labeled at the 5′ end have a number of limitations, including the inability to follow degradation further into the body of the RNA, in the current studies we used a DCP+1 RNA containing a single internal radioactive phosphate. The 39-nucleotide DCP+1 RNA was constructed by ligating an 18-nucleotide upstream fragment (U. Half) with a 5′-labeled, 21-nucleotide downstream fragment (D. Half) (Fig. 1C). The DCP+1 RNA contained a hydroxyl group at the 5′ end and a single radioactive phosphate between residues 17 and 18 of the DCP, near the center of the HDE. Incubation of this RNA in a mouse nuclear extract under standard conditions (20 mM EDTA) resulted in a release of the labeled mononucleotide from the body of the RNA, with a small amount of the product visible after 5 min of incubation (Fig. 1D, lanes 1 to 5). The nuclease functions processively since only relatively small amounts of intermediates were detected during the 60-min reaction. The anti-M oligonucleotide at 10 ng/μl blocked degradation of the DCP+1 substrate, whereas the anti-D oligonucleotide at the same concentration had no effect (Fig. 1D, lanes 6 to 8), demonstrating that nuclease activity depends specifically on binding of the U7 snRNP to the HDE.

In order to release the radioactive nucleotide, the nuclease had to remove nearly half of the HDE that is required to recruit the U7 snRNP. We carried out a competition experiment to determine whether RNAs containing only partial HDE sequences can bind the U7 snRNP and therefore inhibit processing of the H2a-614 pre-mRNA. We used the downstream and the upstream DCP halves (D. Half and U. Half, respectively) (Fig. 1C), each at a 1,000-molar excess over the pre-mRNA substrate. Neither the D. Half nor the U. Half RNAs, containing 9 and 6 nucleotides of the HDE, respectively, affected the processing of the pre-mRNA substrate (Fig. 1E, lanes 5 and 6). In contrast, the same molar excess of the DCP+1 RNA containing the entire HDE prevented cleavage of the H2a-614 pre-mRNA (Fig. 1E, lane 4). Thus, the removal of the first 6 nucleotides of the HDE during the degradation of the DCP likely displaces the U7 snRNP from the RNA substrate. We also tested whether 5′-labeled D. Half and U. Half RNAs can be degraded in a mouse nuclear extract in a U7-dependent manner. Consistent with the inability of partial HDE sequences to bind the U7 snRNP, neither substrate generated U7-dependent degradation products (not shown).

In the above-described experiment, the DCP+1 substrate was labeled internally with a single radioactive phosphate and contained a hydroxyl group at the 5′ end. The fact that this substrate was efficiently degraded demonstrates that the U7-dependent nuclease does not require a phosphate at the 5′ end. To determine whether the addition of a 5′ phosphate can stimulate the degradation efficiency, we incubated the DCP+1 RNA with T4 polynucleotide kinase and unlabeled ATP and tested the resulting 5′ phosphorylated substrate in a nuclear extract. The efficiency of degradation was not significantly increased (not shown), indicating that the U7-dependent nuclease activity does not prefer substrates with a 5′ phosphate.

U7-dependent degradation of RNA substrates containing modified nucleotides upstream of the HDE. The DCP+1 substrate used in our previous studies, referred to here as DCP+1/s_{+1}, contained a phosphorothioate group between the first and the second nucleotides (11). The presence of the modification did not block the release of the 5′-labeled mononucleotide but

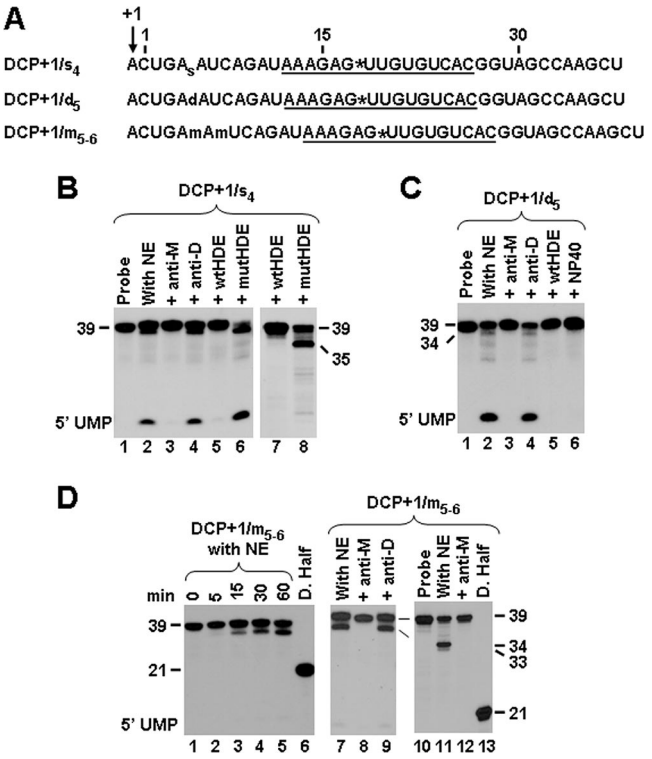

FIG. 2. U7-dependent degradation of RNA substrates containing modified nucleotides upstream of the HDE. (A) Sequence of the DCP+1/s_4, DCP+1/d_5, and DCP+1/m_{5-6} RNA substrates labeled internally with a single radioactive phosphate. The modified positions are indicated with the appropriate letters (s, d, or m), and the radioactive phosphate is indicated with an asterisk. (B) U7-dependent degradation of the DCP+1/s_4 substrate (lanes 1 to 6) in a mouse nuclear extract (NE) under control conditions (lane 2) or in the presence of various RNA competitors, indicated at the top of each lane (lanes 3 to 6). The lengths of the RNA substrates and the positions of labeled mononucleotides are indicated. The RNA products shown in lanes 5 and 6 were additionally resolved by high-resolution gel electrophoresis (lanes 7 and 8; the radioactive mononucleotide is not shown). (C) U7-dependent degradation of the DCP+1/d_5 RNA in a mouse nuclear extract under control conditions (lane 2) or in the presence of various RNA competitors or 0.05% NP-40, as indicated at the top of each lane (lanes 3 to 6). (D) Sixty-minute time course of the U7-dependent degradation of the DCP+1/m_{5-6} RNA in a mouse nuclear extract (lanes 1 to 5) and the effect of the anti-M (lane 8) or anti-D (lane 9) oligonucleotides. The 21-nucleotide downstream-half RNA (D. Half) labeled at the 5′ end is shown in lane 6. High-resolution gel analysis of the DCP+1/m_{5-6} RNA and the degradation products generated under control conditions or in the presence of the anti-M oligonucleotide are shown in lanes 10 to 12.

was absolutely required for cross-linking of the CPSF-73 to the scissile bond by presumably slowing down the rate of catalysis. To determine the effect of the phosphorothioate modification on the activity of the U7-dependent nuclease in more detail, we constructed a DCP+1/s_4 substrate containing a single phosphorothioate bond between nucleotides 4 and 5 of the DCP sequence and a single radioactive phosphate between nucleotides 17 and 18 (Fig. 2A) (see Materials and Methods for the terminology used to name RNA substrates). Under control reaction conditions, about 40% of the input RNA was converted into equal amounts of two labeled products: an intermediate migrating slightly faster than the input RNA and mononucleotides (Fig. 2B, lane 2). High-resolution gel electrophoresis demonstrated that the intermediate is 35 nucleotides long, consistent with the removal of 4 nucleotides prior to the encounter with the modified bond (Fig. 2B, lane 8). The reaction was abolished by the presence of the anti-M oligonucleotide or a 1,000-molar excess of an RNA containing the wild-type HDE (wtHDE), each of which prevents the interaction of the U7 snRNP with the substrate (Fig. 2B, lanes 3 and 5). Surprisingly, the degradation of the DCP+1/s_4 substrate was significantly enhanced by the same molar excess of an RNA bearing a 4-nucleotide substitution within the HDE (mutHDE), although the same proportion of the two products was observed (Fig. 2B, lane 6). This mutant competitor RNA is unable to bind U7 snRNA and to undergo the U7-dependent degradation (11). Our preliminary studies indicate that the stimulatory effect is caused by sequestering an hnRNP protein, which is present in high concentrations in many of our nuclear extracts and may interfere with the recruitment of the U7 snRNP to the HDE (see below).

The degradation pattern of the DCP+1/s_4 substrate demonstrated that the nuclease proceeds from the 5′ end and stalls with a frequency of about 50% at the modified nucleotide, thus behaving as a typical 5′ exonuclease. To further support the 5′-3′ polarity of the U7-dependent nuclease and to characterize its tolerance for other nucleotide modifications, we used the DCP+1/d_5 substrate, containing a single deoxynucleotide at position 5 of the DCP sequence and an internal radioactive phosphate between nucleotides 17 and 18 (Fig. 2A). The degradation of the DCP+1/d_5 RNA resulted in an efficient release of the labeled mononucleotide, and only a small amount of a 34-nucleotide product was detected (Fig. 2C, lane 2), demonstrating that deoxynucleotides are only a minor obstacle for the 5′ exonuclease. The exonuclease activity was inhibited by blocking the U7 snRNA with the anti-M oligonucleotide (Fig. 2C, lane 3) or a 1,000-molar excess of the wtHDE substrate (Fig. 2C, lane 5). Moreover, the reaction was completely abolished by 0.05% NP 40 (Fig. 2C, lane 6), previously shown to inhibit the recruitment of CPSF-73 by the U7 snRNP during endonucleolytic cleavage of histone pre-mRNA (11).

We also replaced the fifth and sixth nucleotides of the DCP sequence in the DCP+1 RNA with their 2′-*O*-methyl analogs, creating the DCP+1/m_{5-6} substrate (Fig. 2A). 2′-*O*-Methyl-modified nucleotides significantly increase the resistance of RNA substrates against a variety of nucleases (20). Incubation of this substrate with a mouse nuclear extract did not yield any mononucleotides and instead resulted in the accumulation of a single product that was shorter by a few nucleotides than the input RNA (Fig. 2D, lanes 1 to 5) but significantly longer than the 21-nucleotide downstream-half RNA corresponding to the last 21 nucleotides of the DCP+1 RNA (Fig. 2D, lane 6). The generation of this product was blocked by the anti-M oligonucleotide (Fig. 2D, lane 8) and was not significantly stimulated by the presence of a 5′ phosphate on the DCP+1/m_{5-6} substrate (not shown). High-resolution gel electrophoresis revealed that the accumulated product was 34 nucleotides long (Fig. 2D, lanes 10 to 13). In addition to this major product, there was also a small amount of a 1-nucleotide-shorter fragment. Thus, the nuclease begins degradation from the 5′ end and stalls predominantly at the first modified nucleotide, with the second modified nucleotide completely preventing further

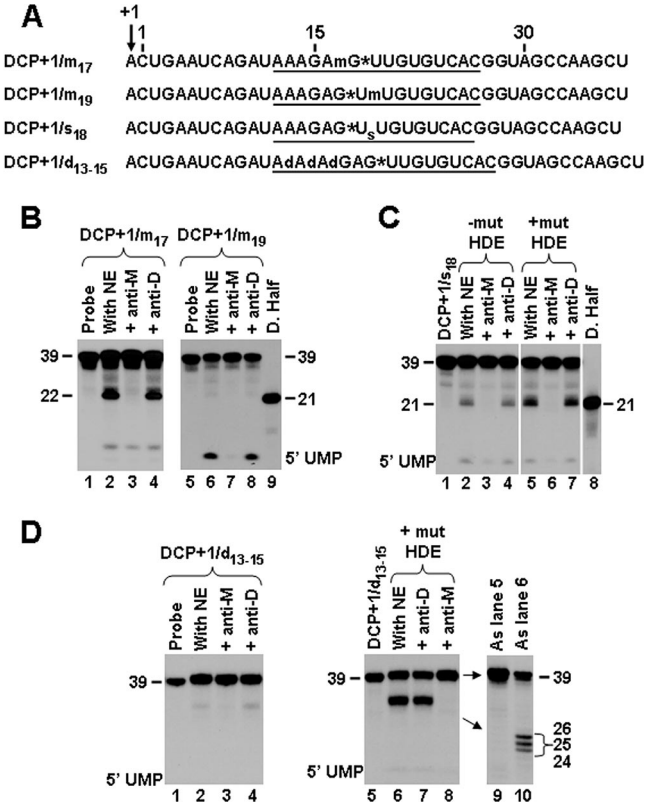

FIG. 3. Effects of modified nucleotides located within the HDE on the U7-dependent degradation. (A) Sequences of the DCP+1/m_{17}, DCP+1/m_{19}, DCP+1/s_{18}, and DCP+1/d_{13-15} substrates labeled internally with a single radioactive phosphate. The HDE is underlined, and the position of the radioactive phosphate is indicated with an asterisk. (B) U7-dependent degradation of the DCP+1/m_{17} (lanes 2 to 4) and DCP+1/m_{19} (lanes 6 to 8) substrates in a mouse nuclear extract (NE) under control conditions (lanes 2 and 6) or in the presence of oligonucleotides blocking the mouse (anti-M; lanes 3 and 7) or *Drosophila* (anti-D, lanes 4 and 8) U7 snRNA. Lane 9 contains the 5′-labeled, 21-nucleotide downstream-half RNA. (C) U7-dependent degradation of the DCP+1/s_{18} RNA in a mouse nuclear extract in the absence (lanes 2 to 4) or in the presence (lanes 5 to 7) of the mutHDE competitor. Lane 8 contains the 5′-labeled, 21-nucleotide downstream-half RNA. (D) U7-dependent degradation of the DCP+1/d_{13-15} RNA in a mouse nuclear extract in the absence (lanes 2 to 4) or in the presence (lanes 6 to 8) of the mutHDE competitor. The RNA samples shown in lanes 5 and 6 were additionally analyzed by high-resolution gel electrophoresis (lanes 9 and 10). Lanes 1 and 5 contain smaller amounts of the substrate.

progression of the enzyme and protecting the downstream labeled sequence. Overall, these experiments provide conclusive evidence that the DCP generated during 3′-end processing of histone pre-mRNAs is degraded 5′ to 3′ by a U7-dependent exonuclease.

Effects of modified residues located within the HDE on U7-dependent degradation. The substrates described above contained modified nucleotides upstream of the HDE. We next incorporated the same modifications within the HDE and tested their effects on the efficiencies of degradation of the resulting substrates. A single 2′-*O*-methyl nucleotide placed in position 17 or 19 of the DCP sequence, i.e., immediately before or after the radioactive phosphate (Fig. 3A), did not affect the overall degradation efficiencies of the respective substrates, DCP+1/m_{17} and DCP+1/m_{19}, indicating that this modification does not interfere with U7 snRNP binding (Fig. 3B, lanes 2 and 6). The degradation pattern of each substrate was consistent with the predicted properties of the U7-dependent exonuclease, which degrades in the 5′-to-3′ direction and stalls at the modified nucleotide. The DCP+1/m_{17} substrate was degraded to an intermediate that migrates slightly slower than the 5′-labeled, 21-nucleotide downstream half (Fig. 3B, lane 9) and, as shown using high-resolution gel electrophoresis, is 22 nucleotides long (see Fig. S1, lane 8, in the supplemental material). The DCP+1/m_{19} substrate has the modified nucleotide 3′ of the radioactive phosphate and yielded labeled 5′ UMP when incubated in the nuclear extract (Fig. 3B, lane 6). As shown for the DCP+1/s_4 substrate (Fig. 2), a 1,000-molar excess of the mutHDE RNA significantly increased the efficiencies of degradation of both the DCP+1/m_{17} (see Fig. S1, lane 3, in the supplemental material) and the DCP+1/m_{19} RNAs (not shown).

Placing a phosphorothioate modification between nucleotides 18 and 19 of the DCP sequence in DCP+1/s_{18} (Fig. 3A) greatly reduced the efficiency of degradation. Small amounts of two labeled products were generated, a 21-nucleotide intermediate and 5′ UMP, with an overall efficiency of about 5% (Fig. 3C, lane 2). This efficiency was only moderately enhanced by a 1,000-molar excess of the mutHDE, which removes a nonspecific inhibitor (Fig. 3C, lane 5). Interestingly, the degradation reaction predominantly yielded the 21-nucleotide product and very few mononucleotides. Thus, a phosphorothioate modification located within the HDE constitutes a much stronger block for the U7-dependent 5′ exonuclease than a phosphorothioate located near the 5′ end (see below). The poor degradation of the DCP+1/s_{18} substrate most likely results from the lower thermal stability of the duplex formed between the modified HDE and the U7 snRNA and thus inefficient recruitment of the 5′ exonuclease to the substrate (7).

We also tested the effect of placing three consecutive deoxynucleotides in positions 13 to 15 in the DCP+1/d_{13-15} RNA (Fig. 3A). Degradation of this substrate under normal reaction conditions was nearly completely inhibited (Fig. 3D, lane 2). However, in contrast to that for the DCP+1/s_{18} substrate, the degradation efficiency for the DCP+1/d_{13-15} substrate was strongly stimulated by the presence of the mutHDE RNA, reaching the level typical of other substrates (Fig. 3D, lane 6). High-resolution gel electrophoresis revealed the presence of three closely migrating intermediates, with lengths of 24, 25, and 26 nucleotides (Fig. 3D, lane 10). This degradation pattern is consistent with the fact that the U7-dependent nuclease partially stalls at the single deoxynucleotide in the DCP+1/d_5 RNA (Fig. 2C) and indicates that three deoxynucleotides within the HDE are sufficient to completely block further progression of the exonuclease, preventing the release of the radioactive mononucleotide. The fact that the DCP+1/d_{13-15} RNA is degraded with the normal efficiency in the presence of the mutHDE indicates that the incorporation of the three deoxynucleotides does not abolish the ability of the HDE to interact with the U7 snRNP and further supports a previous conclusion that the only role of the HDE is to form a sufficiently stable duplex with the U7 snRNA (2, 31). We predict that the three deoxynucleotides within the HDE stimulate in-

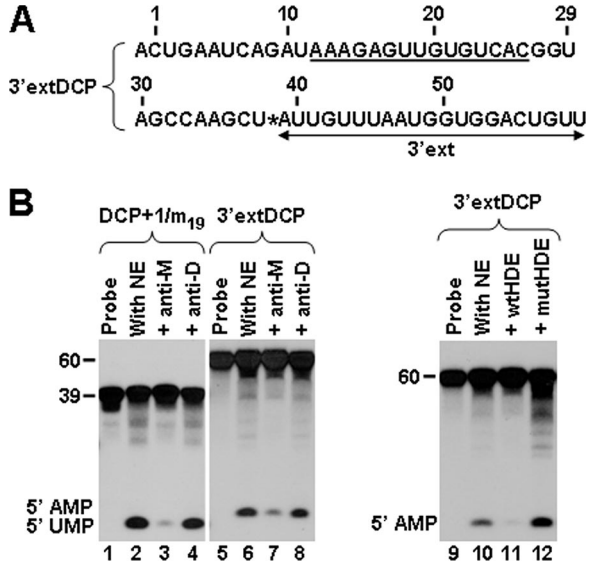

FIG. 4. Degradation of the 3′extDCP RNA containing a single radioactive phosphate downstream of the HDE. (A) Sequence of the 60-nucleotide 3′extDCP RNA. The HDE is underlined, and the position of the radioactive phosphate is indicated with an asterisk. The 3′ext RNA is indicated with a double-arrowed line. (B) U7-dependent degradation of the 3′extDCP RNA under control conditions (lane 6 and 10) or in the presence of various RNA competitors, as indicated at the top of each lane. The degradation efficiency for the DCP+1/m_{19} RNA (Fig. 3A) is shown in lanes 1 to 4 for comparison. NE, nuclear extract.

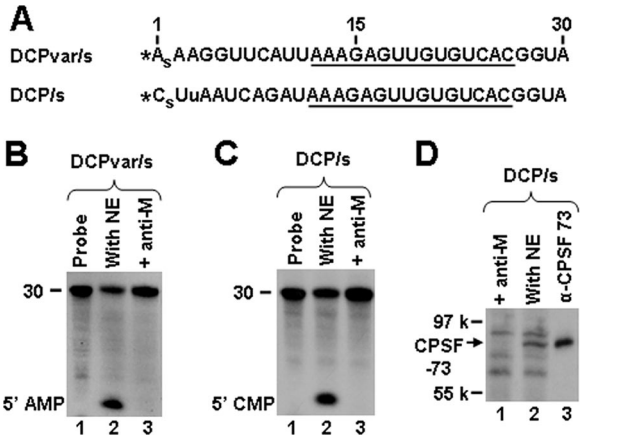

FIG. 5. Detecting U7-dependent interactions during degradation of the DCP. (A) Sequence of the DCPvar/s and DCP/s substrates containing a single radioactive phosphate at the 5′ end (asterisk) and a phosphorothioate modification (s) between nucleotides 1 and 2. (B and C) U7-dependent degradation of the DCPvar/s (B) and DCP/s (C) substrates under control conditions or in the presence of the anti-M oligonucleotide, as indicated at the top of each line. NE, nuclear extract. (D) Formation of the U7-dependent cross-link between CPSF-73 and the scissile bond in the DCP/s substrate. The substrates were incubated with a mouse nuclear extract either under control conditions (lane 2) or in the presence of the anti-M oligonucleotide (lane 1). After brief incubation, the reaction mixtures were UV irradiated, treated with RNase A, and separated on an SDS-polyacrylamide gel. The identity of the CPSF-73 cross-link was confirmed by immunoprecipitation with an anti-CPSF-73 antibody (lane 3).

teraction of the HDE with an inhibitory hnRNP protein and hence cause a poor recruitment of the U7 snRNP in the absence of the mutHDE RNA.

Degradation of a substrate containing a radioactive phosphate downstream of the HDE. The above-described experiments demonstrated that the U7-dependent 5′ exonuclease can remove at least the first 19 nucleotides of the DCP+1 RNA, releasing labeled 5′ UMP. To determine whether the exonuclease can progress further into the body of the RNA substrate to remove the entire U7 binding site, we used a 60-nucleotide substrate (3′extDCP) created by ligating the DCP+1 RNA to a 5′-labeled, 21-nucleotide RNA designated 3′ext. In the 3′extDCP substrate, the only radioactive phosphate was located 12 nucleotides downstream of the 3′ end of the HDE (Fig. 4A). Incubation of the 3′extDCP substrate in a mouse nuclear extract resulted in a U7-dependent accumulation of labeled 5′ AMP, indicating that the 5′ exonuclease can remove at least 40 nucleotides from the 5′ end (Fig. 4B, lane 6), progressing completely through the HDE and displacing the U7 snRNP. Compared to the degradation of the DCP+1/m_{19} (Fig. 4B, lane 2) substrate, the degradation of the 3′extDCP substrate was less efficient. Since the two substrates have the same sequence for the first 39 nucleotides, including the HDE, the most likely explanation for the inefficient degradation of the 3′extDCP is an inhibitory effect of the additional 21 nucleotides located at the 3′ end on the recruitment of the U7 snRNP (see below). As observed for other substrates, the degradation efficiency of the 3′extDCP substrate can be significantly improved by the presence of a high excess of the mutHDE RNA (Fig. 4B, lane 12).

Detecting U7-dependent interactions during degradation of the DCP. To identify proteins that interact with the cleavage site during DCP degradation, we carried out UV cross-linking studies. The RNA substrates used in these studies contained a number of minor changes compared to the DCP+1 substrate used in the above-described studies. First, we established that reducing the number of nucleotides that follow the HDE from 12 to 4 has a stimulatory effect on the efficiency of degradation (not shown). Moreover, instead of using DCP derivatives that were extended at the 5′ end by 1 nucleotide (DCP+1 substrates) we used RNA substrates that began immediately after the cleavage site (DCP substrates). Finally, to have a choice of using either RNase A or RNase T1 in cross-linking studies, we replaced the first guanosine in the DCP with uridine (Fig. 5A). This change was expected to be neutral for the U7-dependent degradation since the region located between the HDE and the cleavage site is not conserved (2). Indeed, we tested an RNA substrate in which this sequence was completely changed (DCPvar/s) and did not observe any changes in the efficiency of degradation (Fig. 5A and B).

To slow down catalysis during degradation and thus allow UV cross-linking of the 5′ exonuclease to the DCP substrate, a phosphorothioate modification (s) was placed in the first phosphodiester bond. This substrate, referred to as DCP/s (Fig. 5A), was degraded in a mouse nuclear extract with an efficiency of about 40% (Fig. 5C, lane 2). To form UV cross-links, the DCP/s RNA was incubated with a mouse nuclear extract for 10 min at 32°C, the time required to initiate degradation. The reaction samples were subsequently UV irradiated, treated with RNase A, and analyzed on SDS gels for the presence of

radioactively labeled proteins. RNase A cleaves the DCP/s RNA immediately after the labeled cytosine (Fig. 5A), thus allowing identification of proteins that interact only with the first scissile bond. A single U7-dependent cross-link migrating at 80 to 85 kDa was readily detected (Fig. 5D, lane 2) and its identity determined by immunoprecipitation with anti-CPSF-73 antibody to be CPSF-73 (Fig. 5D, lane 3). The fact that CPSF-73 was the only protein cross-linked to DCP/s RNA in a U7-dependent manner is consistent with the idea that CPSF-73 functions as the 5′ exonuclease.

Minimal space upstream of the HDE required for exonucleolytic degradation. We asked whether the DCP−9/s RNA, containing only 2 nucleotides upstream of the HDE and a phosphorothioate modification in the first phosphodiester bond (Fig. 6A), could be efficiently degraded by the U7-dependent 5′ exonuclease. Significantly, a 90-min incubation of the 5′-labeled DCP−9/s RNA in a nuclear extract did not yield labeled mononucleotides (Fig. 6B, lane 2). The failure to undergo degradation did not result from the proximity of the phosphorothioate modification to the HDE and poor recruitment of the U7 snRNP, since a molar excess of unlabeled DCP−9/s RNA competed a control degradation reaction with the same efficiency as the full-length DCP (see Fig. S2B in the supplemental material). In addition, extension of the 5′-labeled DCP−9/s RNA by a 14-nucleotide fragment converted the DCP−9/s RNA to a substrate that was efficiently degraded (see Fig. S2C, lane 2, in the supplemental material). From this analysis we conclude that the inability of the DCP−9/s RNA to undergo U7-dependent degradation is caused by an insufficient space upstream of the HDE.

To determine the minimal size of the region located upstream of the HDE that is required to support the degradation process, we tested a set of gradually shortened DCP substrates: DCP−2/s, DCP−4/s, and DCP−7/s (Fig. 6A). Only the DCP−2/s substrate was degraded in the extract by the U7-dependent 5′ exonuclease, whereas the other two substrates were stable (Fig. 6C). The DCP−2/s RNA was reproducibly degraded with lower efficiency (25 to 30% of the input) than the DCP/s RNA, further emphasizing the importance of an optimal length upstream of the HDE. We conclude that substrates containing only 7 nucleotides upstream of the HDE (DCP−4 or shorter) despite containing the entire HDE are not degraded by the U7-dependent 5′ exonuclease. An additional important conclusion from this analysis is that if the U7-dependent 5′ exonuclease dissociated from the RNA substrate after removal of the first 4 nucleotides, it would be unable to act again on the same RNA molecule. The lack of intermediates of this length further supports our initial observation that the 5′ exonuclease acts processively.

We tested whether CPSF-73 can also be UV cross-linked to the modified scissile bond in the DCP−2/s RNA. Compared to all previously tested substrates, the modified bond in the DCP−2/s RNA is located within the body of the DCP and relatively close to the HDE. Importantly, DCP−2/s RNA also formed a U7-dependent cross-link migrating at about 80 kDa (Fig. 6D, bottom, lanes 1 and 3) that was identified by immunoprecipitation as CPSF-73 (not shown). The efficiency of CPSF-73 cross-linking was relatively low due to the suboptimal character of the DCP−2/s RNA, which contains the shortest region upstream of the HDE supporting degradation. We additionally used DCP−2max/s RNA, a derivative of DCP−2/s RNA containing the improved HDE that allows for an uninterrupted 15-bp duplex with the U7 snRNA (Fig. 6 A). As expected, CPSF-73 cross-linked to the DCP−2max/s RNA more efficiently than to the DCP−2/s RNA, reflecting the more stable association of the U7 snRNP (Fig. 6E, bottom, lanes 1 and 3).

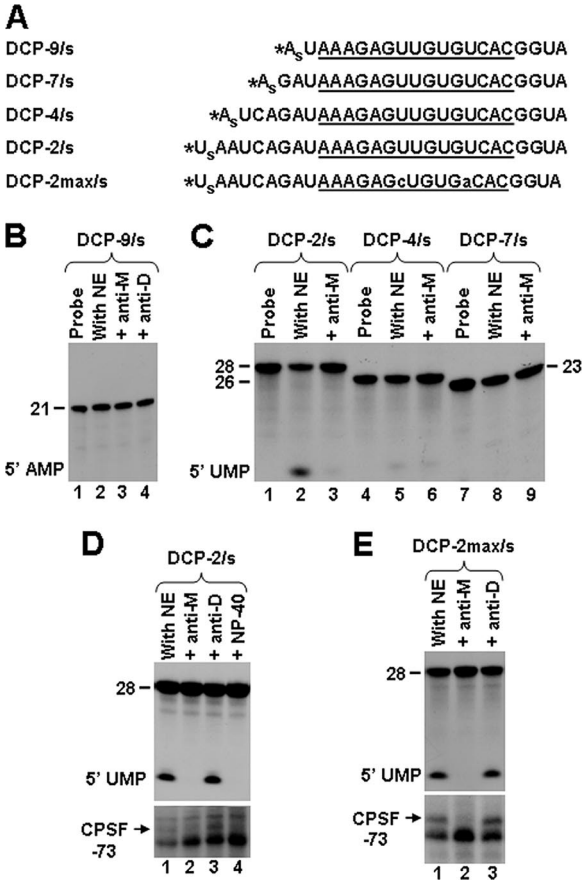

FIG. 6. Minimal space upstream of the HDE required for exonucleolytic degradation. (A) Sequence of the DCP derivatives truncated upstream of the HDE. All substrates were labeled at the 5′ end and contained a phosphorothioate modification (s) between nucleotides 1 and 2. (B) U7-dependent degradation of the DCP−9/s substrate under control conditions or in the presence of the anti-U7 oligonucleotides, as indicated. NE, nuclear extract. (C) U7-dependent degradation of the DCP−2/s, DCP−4/s, and DCP−7/s substrates under control conditions or in the presence of the anti-M oligonucleotide, as indicated. (D) The DCP−2/s and DCPmax/s substrates were analyzed for U7-dependent degradation (top) and UV cross-linking to CPSF-73 (bottom). The reactions were carried out under control conditions or in the presence of the anti-U7 oligonucleotides or NP-40, as indicated. UV cross-linking was performed as explained in the legend to Fig. 5. The position of the CPSF-73 cross-link is indicated with an arrow. (E) The DCP−2max/s substrate was analyzed for U7-dependent degradation (top) and UV cross-linking to CPSF-73 (bottom). The reactions were carried out under control conditions or in the presence of the anti-M oligonucleotide, as indicated.

Switching between the 5′ exonuclease and endonuclease modes. In our previous study, we used a DCP substrate that was extended at the 5′ end by 5 nucleotides and contained a phosphorothioate modification at the cleavage site (11). This substrate, previously called HDE+5/s and renamed here to

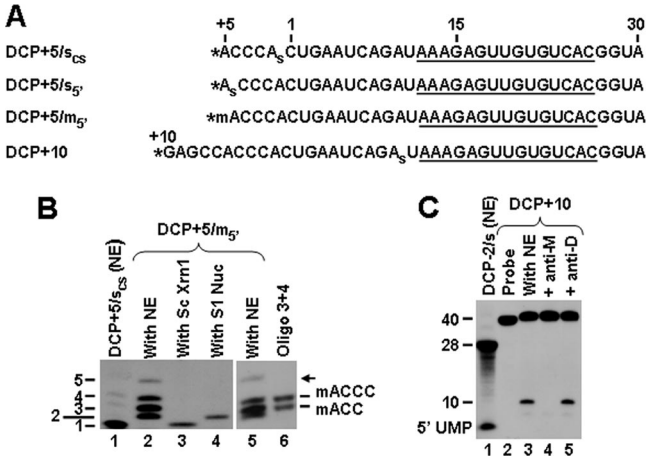

FIG. 7. Switching between the 5′ exonuclease and endonuclease modes. (A) Sequence of DCP derivatives extended at the 5′ end by 5 or more nucleotides and labeled at the 5′ end (asterisk). The positions of phosphorothioate (s) and 2′-*O*-methyl (m) modifications are indicated. (B) High-resolution-gel analysis of the U7-dependent products generated by incubation of the DCP+5/s_{cs} (lane 1) and DCP+5/$m_{5'}$ (lanes 2 and 5) substrates in a mouse nuclear extract (NE). Lanes 3 and 4 contain products of complete digestion of the DCP+5/$m_{5'}$ RNA with the yeast Xrn1 5′ exonuclease and the S1 nuclease, respectively. Lane 6 contains a mixture of two synthetic oligonucleotides labeled at the 5′ end, mACC and mACCC, which serve as size markers. The 5-nucleotide product that results from cleavage at the natural endonucleolytic site is indicated with an arrow. (C) U7-dependent cleavage of the DCP+10 substrate under control conditions or in the presence of the anti-U7 oligonucleotides, as indicated. Degradation of the DCP−2/s (lane 1) substrate is shown to indicate the positions of mononucleotides.

DCP+5/s_{cs} (Fig. 7A), when labeled at the 5′ end and incubated in a mouse nuclear extract yielded labeled mononucleotides diagnostic of the 5′ exonuclease mode (11). There was no detectable 5-nucleotide fragment produced, demonstrating that this substrate is not cleaved endonucleolytically (11). In the nuclear extract used in these studies, incubation of the DCP+5/s_{cs} substrate again predominantly yielded labeled mononucleotides (Fig. 7B, lane 1). One explanation for the predominant 5′ exonucleolytic degradation was that the presence of phosphorothioate at the cleavage site makes endonucleolytic attack by CPSF-73 less favorable than cleavage at the most proximal bond lacking any modification. To test this possibility, we designed a new substrate, DCP+5/$s_{5'}$, containing a phosphorothioate modification at the first phosphodiester bond rather than within the cleavage site (Fig. 7A). This substrate was nearly exclusively cleaved after the first nucleotide, releasing labeled mononucleotides (not shown). These results indicate that CPSF-73 preferentially utilizes the 5′ exonucleolytic mode of its activity if a substrate contains only 5 nucleotides upstream of the cleavage site. To determine whether the predominant cleavage after the first nucleotide results from the inherent inability of the DCP+5 substrate to undergo endonucleolytic cleavage, we next analyzed the pattern of degradation of DCP+5/$m_{5'}$ RNA, in which the first nucleotide was modified by a 2′-*O*-methyl group (Fig. 7A). This modification renders phosphodiester bonds fully resistant to hydrolysis by CPSF-73 and hence was expected to block the 5′ exonuclease activity. The U7-dependent products generated by incubation of this substrate in a nuclear extract were resolved by high-resolution gel electrophoresis next to products of complete digestion of the same RNA by yeast 5′ exoribonuclease Xrn1 and endonuclease S1 (Fig. 7B, lanes 3 and 4). These two nucleases generate a phosphate at the 5′ end, and thus, their products serve as appropriate size markers for the CPSF-73-generated products. To unambiguously determine the sizes of the degradation products, we also used a mixture of two chemically synthesized fragments: mACC and mACCC (Fig. 7B, lane 6). As expected, degradation of the DCP+5/$m_{5'}$ RNA in the nuclear extract did not release labeled mononucleotides and instead generated a group of major U7-dependent products consisting of 2, 3, and 4 nucleotides (Fig. 7B, lane 2). There was also a small amount of a 5-nucleotide product that resulted from hydrolysis at the natural endonucleolytic cleavage site. Interestingly, as judged by the accumulation of labeled mononucleotides, the first phosphodiester bond in the DCP+5/$m_{5'}$ RNA was readily hydrolyzed by Xrn1 (Fig. 7B, lane 3). This could be a biologically relevant feature of Xrn1 5′ exonuclease, as many mRNAs that are degraded by Xrn1 in vivo contain 2′-*O*-methyl-modified nucleotides near the 5′ end as a part of the cap structure. We conclude that CPSF-73 strongly prefers to cleave after the first nucleotide of the DCP+5 RNA, although it is also inherently capable of cleaving this substrate endonucleolytically.

The minimal H2a pre-mRNA substrate that we routinely use to analyze 3′-end processing in vitro contains 38 nucleotides upstream of the cleavage site, including the stem-loop (Fig. 1A). To determine the minimal length upstream of the cleavage site that allows endonucleolytic cleavage, we constructed DCP+10 (Fig. 7A) and DCP+15 (not shown) RNA substrates. In these substrates, the cleavage site was preceded by 10 or 15 nucleotides found in the same position in the H2a pre-mRNA (Fig. 1A). Incubation of the DCP+10 substrate in a mouse nuclear extract yielded a U7-dependent product that migrated significantly slower than mononucleotides (Fig. 7C, lane 3). Generation of the product was blocked by the anti-M oligonucleotide and thus was dependent on the U7 snRNP (Fig. 7C, lane 4). Electrophoresis in a high-resolution gel next to appropriate size markers revealed that DCP+10 was cleaved endonucleolytically at the expected site, generating a 10-nucleotide product (see Fig. S3, lane 5, in the supplemental material). The DCP+15 RNA was also cleaved endonucleolytically, generating a 15-nucleotide-long product (see Fig. S3, lane 3, in the supplemental material). Thus, cleavage is endonucleolytic if the 5′ end of the transcript extends 21 nucleotides from the start of the HDE and exonucleolytic if the 5′ end of the transcript extends between 9 and 16 nucleotides from the start of the HDE.

Xrn2 knockdown stabilizes downstream products in GAPDH (glyceraldehyde-3-phosphate dehydrogenase) but not histone pre-mRNAs in vivo. According to the "torpedo model," degradation of the DCP in the nascent transcript promotes release of RNA polymerase II from the DNA template, resulting in termination of transcription (3, 21, 29, 37). In support of this model, the nuclear 5′-to-3′ exonuclease Xrn2 has been implicated in transcription termination during generation of polyadenylated mRNAs in yeast and mammalian cells (16, 18, 22, 39). Our in vitro results suggest that CPSF-73 rather than Xrn2 could be the 5′ exonuclease that degrades the DCP in histone

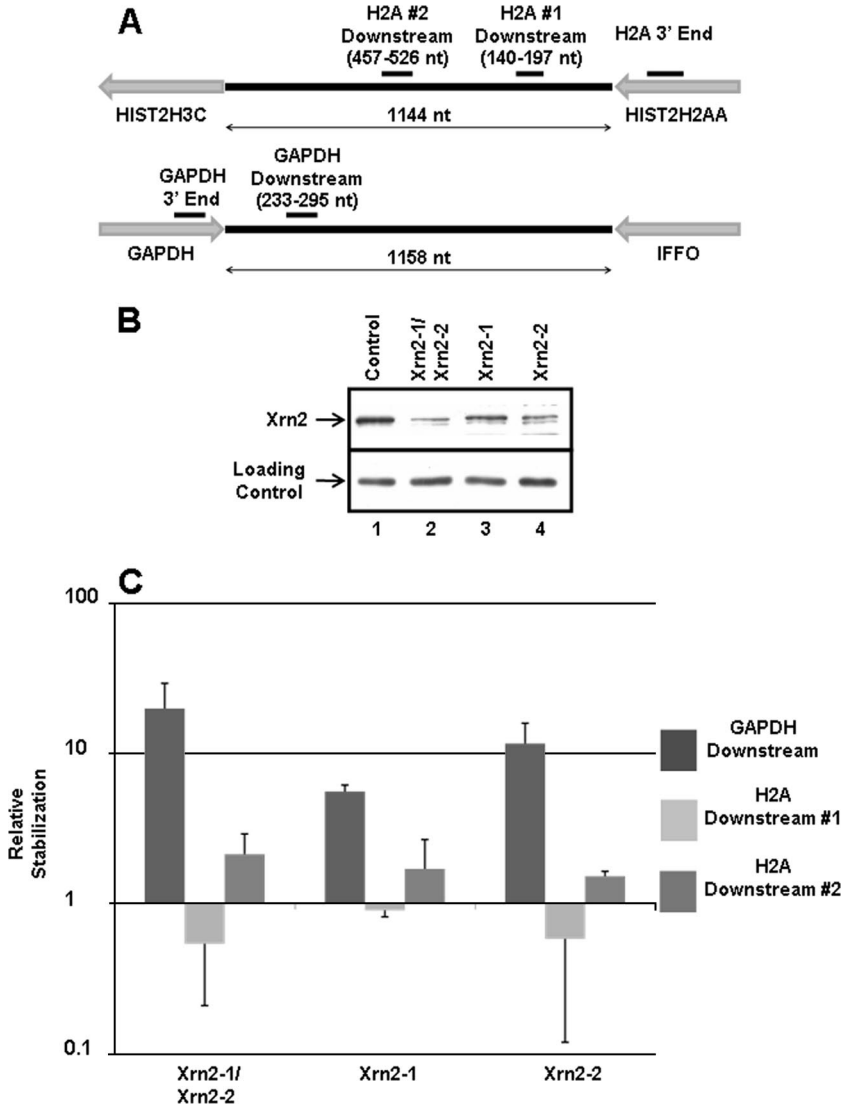

FIG. 8. Xrn2 is not required for degradation of Hist2H2AA DCP in vivo. (A) Probe design for qRT-PCR. Primers were designed to probe regions within the mature mRNAs (3′ End) of both GAPDH and Hist2HAA for normalization purposes. Additional oligonucleotide sets were designed to target regions 140 to 197 nucleotides (nt) and 457 to 526 nucleotides downstream of the Hist2H2AA cleavage site (H2A #1 Downstream and H2A #2 Downstream, respectively) as well as a region 233 to 295 nucleotides downstream of the GAPDH cleavage site (GAPDH downstream). IFFO, intermediate filament family orphan. (B) siRNA-mediated downregulation of Xrn2 in HeLa cells. Individual Xrn2-1 and Xrn2-2 siRNAs (lanes 3 and 4) as well as their combination (lane 2) were used to reduce levels of Xrn2. HeLa cells were collected 72 h after second siRNA transfection and subjected to Western blot analysis using an anti-Xrn2 antibody. A cross-reacting band detected with the Xrn2 antibody serves as the loading control. (C) HeLa cells were treated as in panel B, and RNA was prepared by Trizol extraction. RT reactions were performed using Moloney murine leukemia virus reverse transcriptase and resultant cDNAs subjected to quantitative PCR using the primers described for panel A. Columns represent average stabilization values from three independent experiments, and error bars represent 1 standard deviation.

pre-mRNAs in vivo, potentially promoting termination of transcription on histone genes. To test this hypothesis, we analyzed the effect of knockdown of Xrn2 on accumulation of the DCPs from both the polyadenylated GAPDH transcript and the Hist2H2AA transcript. Each of these genes is quite close to another gene, and hence, transcription termination occurs within ~1,000 nucleotides of the 3′ cleavage site (Fig. 8A). The transcription termination site of the mouse orthologue of the Hist2H2AA gene has been mapped to about 600 nucleotides after the cleavage site (5).

We used two different siRNAs to downregulate Xrn2 in HeLa cells. Each of the two siRNAs significantly reduced Xrn2 levels, although their combination was the most effective (Fig. 8B, lanes 2 to 4). To determine what effect Xrn2 knockdown had on stabilization of downstream products of GAPDH and Hist2H2AA pre-mRNAs, qRT-PCR was performed. We designed oligonucleotide primers that target a region of the GAPDH pre-mRNA 233 to 295 nucleotides downstream from the cleavage site as well as primer sets which target regions 140 to 197 and 457 to 526 nucleotides downstream of the Hist2H2AA cleavage site (Fig. 8A). To determine the amounts of the DCP relative to those of the mature mRNA, we also

used oligonucleotide primers which amplify target sequences upstream of the 3′ cleavage site in each transcript (3′-end regions). Relative amounts of downstream products were determined by comparing the C_T values of downstream PCRs with those of the 3′-end reactions for each knockdown and normalizing these to the values from control siRNA-treated cells. Typically, we observed a difference in C_T values of about eight cycles between the downstream fragment and the 3′ fragment from the mRNA in control cells, implying that the concentration of the downstream fragment was between 0.1 and 1% relative to the mature mRNA. The absolute C_T value for the fragment within both the GADPH and the histone mRNAs (3′ end) varied by less than one cycle among the different samples, indicating that there was not a significant change in either mature mRNA as a result of the siRNA treatments. This analysis allowed us to determine $\Delta\Delta C_T$ values which were used to calculate relative differences in the amounts of downstream products between the knockdown cells and the control cells. Xrn2 knockdown had little effect (<2-fold difference) on the amounts of Hist2H2AA downstream products (Fig. 8C). The distal downstream product displayed a marginal stabilization in all three knockdowns while the proximal downstream product showed a slight destabilization. In contrast, there was a substantial increase in the amount of downstream product from the GAPDH transcript (indicative of its stabilization) in all three knockdowns of Xrn2. Knockdown of Xrn2 with either individual siRNA resulted in a stabilization of between 5- and 10-fold, while the combination knockdown revealed a >15-fold stabilization on average (Fig. 8C), consistent with the degree of knockdown of Xrn2 observed by Western blotting. Taken together, these data indicate that the Xrn2 is involved in the degradation of the GAPDH downstream product but not the Hist2H2AA downstream products. This is consistent with the possibility that after cleavage of the histone pre-mRNA, the 5′ exonuclease activity of CPSF-73 (and not Xrn2) is involved in degradation of the downstream product. Note that knockdown of any component of the 3′-end-processing machinery would result in the increase of the downstream fragment due to a failure to process the pre-mRNA, and hence, direct analysis of the effect of knocking down CPSF-73 is not possible.

DISCUSSION

The U7-dependent nuclease degrades the DCP in the 5′-to-3′ direction and stalls at modified nucleotides. Histone pre-mRNAs are cleaved at the 3′ end by a multicomponent processing machinery that includes the U7 snRNP bound to a region downstream of the cleavage site (10). Following cleavage in vitro, the DCP is rapidly degraded to mononucleotides by a nuclease that also depends on the U7 snRNP. To demonstrate that degradation is carried out by a 5′-to-3′ exoribonuclease, we incorporated differently modified nucleotides into specific sites in the DCP RNA: 2′-*O*-methyl nucleotides, deoxynucleotides, and phosphorothioate nucleotides. Each modification resulted in the accumulation of intermediate products whose sizes clearly demonstrated that degradation begins from the 5′ end and stalls at the modified nucleotide; thus, it behaves as a typical 5′ exonuclease. The strongest block was created by a 2′-*O*-methyl modification, which nearly completely stopped progression of the exonuclease. A single deoxynucleotide located in the same position was relatively well tolerated by the U7-dependent exonuclease, whereas the phosphorothioate modification had an intermediate ability to block the degradation of the DCP.

The U7-dependent 5′ exonuclease activity is processive and proceeds past the HDE, suggesting that it can readily displace the U7 snRNP from the substrate. Thus, binding of the U7 snRNP to the HDE is required only to recruit the 5′ exonuclease and initiate degradation. It is not known whether the exonuclease acts by itself to displace the U7 snRNP or requires assistance from other proteins present in the nuclear extract. However, given that the reaction occurs in the presence of EDTA, the involvement of a conventional helicase in unwinding the RNA duplex formed between the U7 snRNA and the HDE seems unlikely.

Two observations argue against the possibility that in vitro degradation of the DCP in histone pre-mRNA is carried out by the two known and closely related 5′ exonucleases, Xrn1 and Xrn2. First, both enzymes depend on divalent ions and are completely inactivated by low concentrations of EDTA (32, 35). Second, the 5′ exonuclease activity of Xrn1 or Xrn2 requires the presence of a 5′ phosphate (32–35). UV cross-linking studies strongly suggest that the DCP in histone pre-mRNA is degraded by CPSF-73, which was the only U7-dependent protein detected in the vicinity of the first scissile bond during degradation of both the DCP and the DCP−2/s RNAs. Moreover, the U7-dependent activity degrading the DCP in histone pre-mRNA shares a number of similarities with the activity of RNase J1, which, together with CPSF-73, belongs to the β-CASP subfamily of the metallo-β-lactamase proteins (4, 9, 23). RNase J1 was initially characterized as an endonuclease involved in processing of mRNA precursors in *Bacillus subtilis* (14) and subsequently shown to also function as a 5′-to-3′ exonuclease in mRNA degradation and rRNA processing (24). Altogether, this analysis strongly supports the notion that CPSF-73 possesses both endonuclease and 5′ exonuclease activities.

In contrast to our results, a bacterially expressed N-terminal fragment of human CPSF-73 functions only as an endonuclease and fails to degrade RNA substrates in the 5′-to-3′ direction (23). One explanation is that the 5′ exonuclease activity of CPSF-73 requires the assistance of a second component of the processing complex and can be observed only in nuclear extracts or reconstituted systems. It is also possible that the 5′ exonuclease (but not the endonuclease) activity of CPSF-73 vitally depends on the C-terminal portion of the protein. This interpretation is supported by recent crystallographic studies, which demonstrated the importance of the C-terminal domain for the activity of RNase J1 (8).

Previously, an activity that degrades the DCP during histone pre-mRNA processing has been identified in mammalian nuclear extracts by Walther et al. (38). In contrast to our results, this activity stalled at guanine nucleotides and hence generated a family of fragments trimmed at the 5′ end rather than mononucleotides. Further studies are required to determine its relation to CPSF-73, although the dependence on the U7 snRNP and resistance to EDTA suggest that the two activities represent the same enzyme.

The distance of the 5′ end of the substrate from the HDE determines whether CPSF-73 acts as an endonuclease or a 5′ exonuclease. Truncated DCP substrates containing 7 or fewer nucleotides upstream of the HDE are not degraded by CPSF-73, yet they bind the U7 snRNP with normal efficiency. Extending the sequence 5′ of the HDE to 9 nucleotides resulted in a substrate that is degraded, but at a lower efficiency than the normal DCP substrate containing 11 nucleotides in this region. The sequence upstream of the HDE can be changed without a major adverse effect on the degradation efficiency, demonstrating that the sufficient space rather than a specific sequence is critically important. These results are consistent with the fact that in natural histone pre-mRNAs, the region between the HDE and the cleavage site consists of at least 9 nucleotides and is not conserved at the sequence level (2). Our preliminary cross-linking experiments revealed that the region upstream of the HDE interacts in a U7-dependent manner with a group of proteins (unpublished results), which are likely involved in recruiting and/or activating CPSF-73.

Surprisingly, a DCP derivative extending 16 nucleotides 5′ of the start of the HDE (DCP+5 RNA) and thus containing the normal endonucleolytic cleavage site was also degraded from the 5′ end. Endonucleolytic cleavage of this substrate was activated by blocking the 5′ end of the DCP+5 RNA with a 2′-*O*-methyl group. Thus, CPSF-73 preferentially uses the 5′ exonuclease mode on the DCP+5 RNA, although it is intrinsically capable of cleaving this substrate endonucleolytically. Interestingly, as many as four major sites located close to the 5′ end were cleaved upon blockage of the 5′ end of the DCP+5 substrate, with the natural cleavage site being used only rarely. Thus, the processing complex assembled on the DCP+5 substrate leaves CPSF-73 flexibility in selecting sites for endonucleolytic cleavage. Importantly, exclusive cleavage at the correct site was achieved by adding 5 more nucleotides to the 5′ end of the DCP+5 RNA (DCP+10 substrate) instead of blocking this end by a 2′-*O*-methyl group. Perhaps, the region upstream of the cleavage site in the DCP+10 substrate is sufficiently long to interact with a component of the processing machinery, which may stabilize CPSF-73, directing cleavage to the correct site. An important role in preventing the 5′ exonuclease mode in processing of the DCP+10 RNA may also be played by the fact that the 5′ end is located too far away from the HDE and is thus not easily accessible to CPSF-73.

Xrn2 is not required for degradation of the DCP in histone pre-mRNA in vivo. Recent in vivo and in vitro studies demonstrated that the degradation of the DCP during cleavage/polyadenylation involves the well-characterized 5′ exonuclease Xrn2 (16, 18, 22, 39). We demonstrated that downregulation of Xrn2 by RNAi does not result in significant stabilization of the DCP generated from the Hist2H2AA transcript, while, as expected, the corresponding product from the transcript encoding GAPDH was stabilized in the same cells, in agreement with previous studies of polyadenylated mRNAs (15, 39). Thus, it is likely that the 5′ exonuclease activity of CPSF-73 degrades the DCP in histone pre-mRNA also in vivo while the same function for all other protein-encoding transcripts is carried out by Xrn2. The difference may reflect the fact that 3′-end processing of conventional pre-mRNAs is directed by the upstream AAUAAA signal, which recruits CPSF subunits, including CPSF-73 (26), whereas in 3′-end processing of histone pre-mRNA, the recruitment of CPSF-73 critically depends on the downstream HDE, which interacts with the U7 snRNP. Following processing of histone pre-mRNA, CPSF-73 likely remains associated with the U7 snRNP and is perfectly positioned to use its preferential 5′ exonuclease activity to degrade the DCP. It is possible that Xrn2 plays a supportive role, for example, by continuing degradation of the DCP after dissociation of CPSF-73 from the substrate. This interpretation is consistent with our in vivo results demonstrating that the most distal region of the histone transcript is moderately stabilized by siRNA-mediated depletion of Xrn2 while the upstream fragment is not.

One obvious function for the 5′ exonuclease activity of CPSF-73 in vivo may be to degrade the region immediately downstream of the cleavage site and therefore to liberate the U7 snRNP from its base pairing association with the HDE for another round of 3′-end processing, as previously suggested (38). In addition, an attractive possibility is that CPSF-73 continues degradation into more-downstream regions of the nascent histone pre-mRNA, ultimately resulting in displacement of RNA polymerase II from the DNA template and termination of transcription, as postulated for Xrn2 in the torpedo mechanism (3, 21, 29, 37). Indeed, mutations within the 3′-end-processing elements in histone pre-mRNAs (the stem-loop and the HDE) prevent transcription termination in vivo (5), suggesting that as in cleavage/polyadenylation (3), 3′-end processing of histone pre-mRNA is functionally linked to the release of RNA polymerase II from histone genes.

ACKNOWLEDGMENTS

We thank L. Benard and C. Condon (CNRS, Paris, France) for yeast Xrn1 and D. Bentley (University of Colorado) for antibody against CPSF-73. We also thank C. Condon and A. Marchfelder (Ulm University) for comments on the manuscript.

This work was supported by NIH grant GM29832.

REFERENCES

1. **Aravind, L.** 1999. An evolutionary classification of the metallo-beta-lactamase fold proteins. In Silico Biol. **1:**69–91.
2. **Bond, U. M., T. A. Yario, and J. A. Steitz.** 1991. Multiple processing-defective mutations in a mammalian histone premessenger RNA are suppressed by compensatory changes in U7 RNA both in vivo and in vitro. Genes Dev. **5:**1709–1722.
3. **Buratowski, S.** 2005. Connections between mRNA 3′ end processing and transcription termination. Curr. Opin. Cell Biol. **17:**257–261.
4. **Callebaut, I., D. Moshous, J. P. Mornon, and J. P. De Villartay.** 2002. Metallo-beta-lactamase fold within nucleic acids processing enzymes: the beta-CASP family. Nucleic Acids Res. **30:**3592–3601.
5. **Chodchoy, N., N. B. Pandey, and W. F. Marzluff.** 1991. An intact histone 3′ processing site is required for transcription termination in a mouse histone H2a gene. Mol. Cell. Biol. **11:**497–509.
6. **Colgan, D. F., and J. L. Manley.** 1997. Mechanism and regulation of mRNA polyadenylation. Genes Dev. **11:**2755–2766.
7. **Cotten, M., B. Oberhauser, H. Brunar, A. Holzner, G. Issakides, C. R. Noe, G. Schaffner, E. Wagner, and M. L. Birnstiel.** 1991. 2′-O-methyl, 2′-O-ethyl oligoribonucleotides and phosphorothioate oligodeoxyribonucleotides as inhibitors of the *in vitro* U7 snRNP-dependent mRNA processing event. Nucleic Acids Res. **19:**2629–2635.
8. **de la Sierra-Gallay, I. L., L. Zig, A. Jamalli, and H. Putzer.** 2008. Structural insights into the dual activity of RNase J. Nat. Struct. Mol. Biol. **15:**206–212.
9. **Dominski, Z.** 2007. Nucleases of the metallo-beta-lactamase family and their role in DNA and RNA metabolism. Crit. Rev. Biochem. Mol. Biol. **42:**67–93.
10. **Dominski, Z., and W. F. Marzluff.** 2007. Formation of the 3′ end of histone mRNA: getting closer to the end. Gene **396:**373–390.
11. **Dominski, Z., X. C. Yang, and W. F. Marzluff.** 2005. The polyadenylation factor CPSF-73 is involved in histone-pre-mRNA processing. Cell **123:**37–48.
12. **Dominski, Z., X. C. Yang, M. Purdy, and W. F. Marzluff.** 2005. Differences and similarities between *Drosophila* and mammalian 3′ end processing of histone pre-mRNAs. RNA **11:**1835–1847.

13. **Dominski, Z., L. X. Zheng, R. Sanchez, and W. F. Marzluff.** 1999. Stem-loop binding protein facilitates 3′-end formation by stabilizing U7 snRNP binding to histone pre-mRNA. Mol. Cell. Biol. **19:**3561–3570.
14. **Even, S., O. Pellegrini, L. Zig, V. Labas, J. Vinh, D. Brechemmier-Baey, and H. Putzer.** 2005. Ribonucleases J1 and J2: two novel endoribonucleases in B.subtilis with functional homology to E.coli RNase E. Nucleic Acids Res. **33:**2141–2152.
15. **Gromak, N., S. West, and N. J. Proudfoot.** 2006. Pause sites promote transcriptional termination of mammalian RNA polymerase II. Mol. Cell. Biol. **26:**3986–3996.
16. **Kaneko, S., O. Rozenblatt-Rosen, M. Meyerson, and J. L. Manley.** 2007. The multifunctional protein p54nrb/PSF recruits the exonuclease XRN2 to facilitate pre-mRNA 3′ processing and transcription termination. Genes Dev. **21:**1779–1789.
17. **Kaufmann, I., G. Martin, A. Friedlein, H. Langen, and W. Keller.** 2004. Human Fip1 is a subunit of CPSF that binds to U-rich RNA elements and stimulates poly(A) polymerase. EMBO J. **23:**616–626.
18. **Kim, M., N. J. Krogan, L. Vasiljeva, O. J. Rando, E. Nedea, J. F. Greenblatt, and S. Buratowski.** 2004. The yeast Rat1 exonuclease promotes transcription termination by RNA polymerase II. Nature **432:**517–522.
19. **Kolev, N. G., and J. A. Steitz.** 2005. Symplekin and multiple other polyadenylation factors participate in 3′-end maturation of histone mRNAs. Genes Dev. **19:**2583–2592.
20. **Lamond, A. I., and B. S. Sproat.** 1993. Antisense oligonucleotides made of 2′-O-alkylRNA: their properties and applications in RNA biochemistry. FEBS Lett. **325:**123–127.
21. **Luo, W., and D. Bentley.** 2004. A ribonucleolytic rat torpedoes RNA polymerase II. Cell **119:**911–914.
22. **Luo, W., A. W. Johnson, and D. L. Bentley.** 2006. The role of Rat1 in coupling mRNA 3′-end processing to transcription termination: implications for a unified allosteric-torpedo model. Genes Dev. **20:**954–965.
23. **Mandel, C. R., S. Kaneko, H. Zhang, D. Gebauer, V. Vethantham, J. L. Manley, and L. Tong.** 2006. Polyadenylation factor CPSF-73 is the pre-mRNA 3′-end-processing endonuclease. Nature **444:**953–956.
24. **Mathy, N., L. Benard, O. Pellegrini, R. Daou, T. Wen, and C. Condon.** 2007. 5′-to-3′ exoribonuclease activity in bacteria: role of RNase J1 in rRNA maturation and 5′ stability of mRNA. Cell **129:**681–692.
25. **Moore, M. J., and C. C. Query.** 2000. Joining of RNAs by splinted ligation. Methods Enzymol. **317:**109–123.
26. **Murthy, K. G. K., and J. L. Manley.** 1995. The 160-kD subunit of human cleavage polyadenylation specificity factor coordinates pre-mRNA 3′-end formation. Genes Dev. **9:**2672–2683.
27. **Pillai, R. S., M. Grimmler, G. Meister, C. L. Will, R. Luhrmann, U. Fischer, and D. Schumperli.** 2003. Unique Sm core structure of U7 snRNPs: assembly by a specialized SMN complex and the role of a new component, Lsm11, in histone RNA processing. Genes Dev. **17:**2321–2333.
28. **Pillai, R. S., C. L. Will, R. Lührmann, D. Schümperli, and B. Müller.** 2001. Purified U7 snRNPs lack the Sm proteins D1 and D2 but contain Lsm10, a new 14 kDa Sm D1-like protein. EMBO J. **20:**5470–5479.
29. **Rosonina, E., S. Kaneko, and J. L. Manley.** 2006. Terminating the transcript: breaking up is hard to do. Genes Dev. **20:**1050–1056.
30. **Ryan, K., O. Calvo, and J. L. Manley.** 2004. Evidence that polyadenylation factor CPSF-73 is the mRNA 3′ processing endonuclease. RNA **10:**565–573.
31. **Scharl, E. C., and J. A. Steitz.** 1996. Length suppression in histone messenger RNA 3′-end maturation: processing defects of insertion mutant premessenger RNAs can be compensated by insertions into the U7 small nuclear RNA. Proc. Natl. Acad. Sci. USA **93:**14659–14664.
32. **Solinger, J. A., D. Pascolini, and W. D. Heyer.** 1999. Active-site mutations in the Xrn1p exoribonuclease of *Saccharomyces cerevisiae* reveal a specific role in meiosis. Mol. Cell. Biol. **19:**5930–5942.
33. **Stevens, A.** 1978. An exoribonuclease from Saccharomyces cerevisiae: effect of modifications of 5′ end groups on the hydrolysis of substrates to 5′ mononucleotides. Biochem. Biophys. Res. Commun. **81:**656–661.
34. **Stevens, A.** 1980. Purification and characterization of a Saccharomyces cerevisiae exoribonuclease which yields 5′-mononucleotides by a 5′ leads to 3′ mode of hydrolysis. J. Biol. Chem. **255:**3080–3085.
35. **Stevens, A., and T. L. Poole.** 1995. 5′-exonuclease-2 of Saccharomyces cerevisiae. Purification and features of ribonuclease activity with comparison to 5′-exonuclease-1. J. Biol. Chem. **270:**16063–16069.
36. **Takagaki, Y., and J. L. Manley.** 2000. Complex protein interactions within the human polyadenylation machinery identify a novel component. Mol. Cell. Biol. **20:**1515–1525.
37. **Tollervey, D.** 2004. Molecular biology: termination by torpedo. Nature **432:**456–457.
38. **Walther, T. N., K. T. Wittop, D. Schümperli, and B. Muller.** 1998. A 5′-3′ exonuclease activity involved in forming the 3′ products of histone pre-mRNA processing in vitro. RNA **4:**1034–1046.
39. **West, S., N. Gromak, and N. J. Proudfoot.** 2004. Human 5′→3′ exonuclease Xrn2 promotes transcription termination at co-transcriptional cleavage sites. Nature **432:**522–525.
40. **Zhao, J., L. Hyman, and C. Moore.** 1999. Formation of mRNA 3′ ends in eukaryotes: mechanism, regulation, and interrelationships with other steps in mRNA synthesis. Microbiol. Mol. Biol. Rev. **63:**405–445.